Effect of THF on Equilibrium Pressure and Dissociation Enthalpy of CO_2 Hydrates Applied to Secondary Refrigeration

Anthony Delahaye,* Laurence Fournaison, Sandrine Marinhas, and Imen Chatti

Cemagref-GPAN, Parc de Tourvoie, B.P. 44, 92163 Antony Cedex, France

Jean-Pierre Petitet

LIMHP−CNRS, Institut Galilée, Av. J.B. Clément, 93430 Villetaneuse, France

Didier Dalmazzone and Walter Fürst

ENSTA, 32 bd Victor, 75015 Paris, France

The present work investigates the formation conditions and the latent heat of dissociation of hydrates formed from tetrahydrofuran (THF)−CO_2−water mixtures. The conditions investigated are 3.8−15 wt % for THF concentration and 0.2−3.5 MPa for the CO_2 partial pressure range, conditions that are adapted to the use of the corresponding hydrate slurries as secondary refrigerants. Both differential thermal analysis (DTA) and differential scanning calorimetry (DSC) methods were used for the experimental determinations. Experimental values were compared with modeling, combining the van der Waals and Platteeuw approach with the Redlich−Kwong equation of state associated to a modified Huron−Vidal (MHV2) mixing rule. At fixed temperature, adding THF to the systems results in a drastic reduction of CO_2 equilibrium pressure. For instance, at 280 K, a 78.9% decrease of CO_2 pressure is experimentally observed if the solution contains 3.8 wt % of THF. Furthermore, a dissociation enthalpy of (CO_2 + THF) hydrates roughly two times higher that that of CO_2 hydrates was calculated from measured and predicted data of hydrate formation.

1. Introduction

The development of secondary refrigeration is a solution to reduce the use of CFC-type and HFC-type primary refrigerants, progressively banished since the Kyoto Protocol (entered into force on 16 February, 2005). In fact, the use of an environmentally friendly secondary fluid, which is a harmless medium of cold transport to places of use, allows the containment of the primary refrigerant in the engine room. Moreover, solid−liquid secondary refrigerants, made of solid particles (phase-change material) in suspension in the carrying liquid, can improve the energy efficiency of the global refrigerating system thanks to the latent heat of fusion of the solid phase. The most usual two-phase secondary refrigerants are currently ice slurries, but their generators are power-limited because they use mechanical technologies (scraped or brushed-surface heat exchangers). Secondary refrigeration studies can, thus, be directed toward nonmechanical generation.

Hydrate slurries have the advantage of being produced by a nonmechanical process of gas injection in a cooled liquid phase. Nevertheless, the use of hydrate slurries in refrigeration partly requires a high latent heat of dissociation and appropriate (*T*, *P*) stability conditions of hydrate crystals. The objective of the present study is to investigate the impact of tetrahydrofuran (THF) molecules on CO_2 hydrates with the aim of producing hydrate slurries suitable for secondary refrigeration.

As pointed out in the literature,[1] structure II hydrates have a dissociation enthalpy approximately two times higher than that of structure I hydrates. According to other authors,[2] small amounts of THF can change the structure I of mixed (CO_2 + N_2) hydrate[3] to structure II. In addition, previous works carried out on single CO_2 hydrate[4,5] confirmed a dissociation enthalpy of structure I CO_2 hydrate of ∼500 kJ/kg, higher than that of ice (333 kJ/kg). Relying on the previously cited study,[2] the opportunity of changing structure I of CO_2 hydrate to structure II by adding THF might increase its dissociation enthalpy.

THF hydrate was already investigated for air conditioning applications,[6,7] since its phase-change temperature is 277.55 K at atmospheric pressure.[8] At this temperature, the phase-change pressure of CO_2 hydrate is roughly 2.1 MPa, and thus, it is difficult to implement CO_2 hydrate as a secondary refrigerant in classical installations. Relying on the friendly (*T*, *P*) stability field of THF hydrate, mixed hydrates formed from water−THF−CO_2 systems are likely to appear at lower pressures than single CO_2 hydrates.

In the present paper, hydrate formation conditions were measured, using differential thermal analysis (DTA) and differential scanning calorimetry (DSC) devices, on water−THF systems[9−11] and water−THF−CO_2 systems. Hydrate-formation modeling based on the van der Waals and Platteeuw model[12] combined with a predictive equation of state was also developed for the same aqueous systems. Hydrate dissociation enthalpies were estimated using the Clausius−Clapeyron equation[13] based on experimental and modeled equilibrium data.

2. Material and Methods

2.1. DTA Device and Experimental Protocol of Hydrate Formation/Dissociation Study. A previously described experimental DTA device[4] was used to characterize the thermal behavior of water−THF−CO_2 mixtures. It was mainly composed of a glass cell (diameter = 30 mm, volume = 46 cm^3) containing the mixture to be studied and another similar cell containing an inert solution in the same conditions. Solutions were submitted to temperature ramps using the cooling/heating

* To whom correspondence should be addressed. Tel.: +33 (0)140 96 60 21. Fax: +33 (0)140 96 60 75. E-mail: anthony.delahaye@cemagref.fr.

10.1021/ie050356p CCC: $33.50
Published on Web 11/08/2005

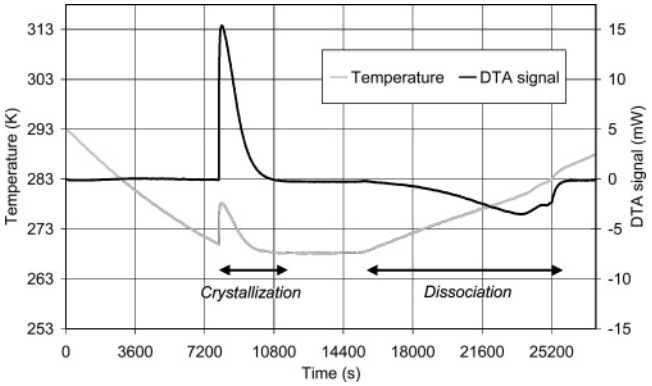

Figure 1. Temperature and DTA signal history during a cycle of crystallization/dissociation of hydrates formed from water−THF−CO_2 systems.

system. A CO_2 injection system was used to set the initial pressure in the cells. Temperature (250−290 K) and pressure (0−4 MPa) were measured using a T-type thermocouple in each cell and two transducers, respectively. DTA analysis was performed from the temperature difference between the two cells measured by 8 T-type thermocouples connected in series.

The L_w-H-V equilibrium conditions of hydrates formed from water−THF−CO_2 systems were measured by a cooling−heating cycle applied to water−THF−CO_2 systems (Figure 1). Hydrate crystallization was caused by a stirring action, as illustrated by the increasing peaks of the temperature and DTA curves. The solid melting was carried out at a heating rate of +0.1 K/min. At this rate, the temperature measured at the end of the hydrate dissociation, corresponding to the top of the second melting peak of the DTA signal, can be considered as a satisfactory approximation of the phase-change temperature of the hydrate. In fact, tests at lower rates than +0.1 K/min give the same results.

2.2. DSC Device and Experimental Protocol of Hydrate Formation/Dissociation Study. The samples were made using freshly distilled water degassed under vacuum. Synthesis-grade THF from SDS (purity = 99.5 wt %) was distilled on sodium to ensure perfect dryness and was kept under vacuum. Two differential scanning calorimeters from Setaram (Lyon, France) were used for the experiments: a μDSC VII for atmospheric pressure measurements and a DSC 111 equipped with pressure-controlled vessels for measurements under pressure of CO_2 (AirLiquide, purity = 99.995 vol %). The experimental set up is presented in Figure 2. The gas pressure was kept constant during the experiments using a 100-DM-model syringe pump from Isco, with an internal volume of 100 mL, and the pressure was measured by a pressure gauge from Bourdon-Sedeme (0−16 MPa), with a resolution of 0.01 MPa.

In DSC experiments, the formation of the composite (CO_2 + THF) hydrate is in competition with both the crystallization of ice and the formation of single hydrates of CO_2 and/or THF. Given the experimental conditions, if water content does not exceed the quantity needed to form the composite (CO_2 + THF) hydrate, this composite hydrate is the only stable solid phase. If water is in excess, the stable solid phases are the composite (CO_2 + THF) hydrate and also the single CO_2 hydrate.

However, the formation of both hydrates requires the transport of CO_2 from the gas phase into the liquid phase, which can only be made by diffusion and natural convection since no agitation is provided. On the contrary condition, ice and single THF hydrate readily crystallize with no need for gas diffusion. For this reason, in the case of water−THF−CO_2 systems, ice and single THF hydrate may actually be present and consume

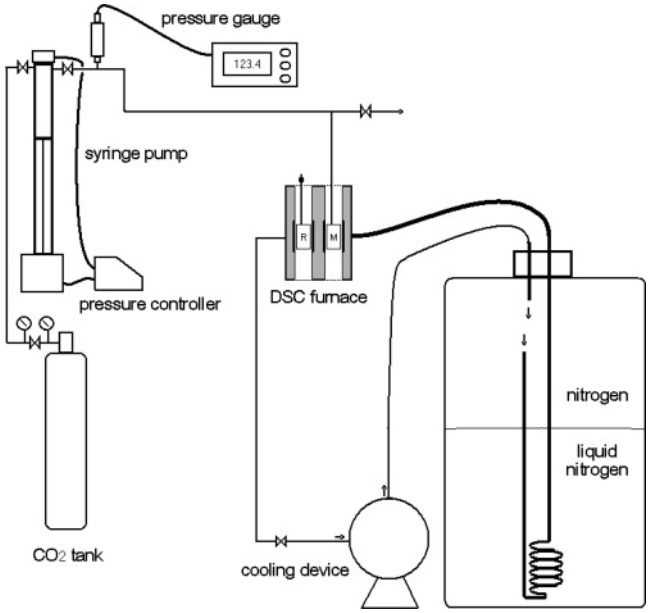

Figure 2. DSC device: R, reference vessel; M, sample vessel.

the majority of the available water. To enhance the yield of conversion to CO_2-containing hydrates, successive cooling and warming sequences were applied to the samples in a range of temperatures that was adjusted to successively crystallize and melt ice and single THF hydrate and to allow the more-stable hydrates, i.e., CO_2 hydrate and (CO_2 + THF) hydrate, to accumulate at each cycle. Examples of thermograms recorded at two different pressures are presented in Figure 3. The sample was a 5.97 wt % THF solution, in which water was in excess with respect to the theoretical hydrate composition (19.07 wt %). It can be noticed that the areas of crystallization and melting peaks regularly decrease during the three or four first cycles. The following heat signals do not present any noticeable change, suggesting that the amount of (CO_2 + THF) hydrate reached a maximum. A slower warming program (+0.5 K/min) was then applied until complete dissociation of the hydrates, which appeared in the form of two peaks, having the shape of a eutectic melting peak followed by a progressive melting peak. It was assumed that this signal was attributable to the dissociation of a mixture of CO_2 hydrate and (CO_2 + THF) hydrate. The (T, P) equilibrium points for (CO_2 + THF) hydrate were taken at the temperature that corresponds to the end of the progressive melting, i.e., the top of the progressive dissociation peak. In addition, measurements were made at atmospheric pressure on THF hydrate, where no problem of competition with ice crystallization was encountered.

2.3. Modeling of Hydrate Formation in the Water−THF−CO_2 System. The modeling of hydrate formation in the water−THF−CO_2 system was carried out by combining the van der Waals and Platteeuw model[12] with a predictive equation of state. The choice of using a predictive expression for the excess properties involved in the calculation of hydrate-stability conditions is justified by the fact that we intend to use the model to formulate the hydrate slurries used as secondary refrigerants. The prediction of the effect resulting from adding new compounds to the system will allow us to get adapted stability conditions. The equilibrium condition may be expressed through the equality of water chemical potential in the liquid phase and in the hydrate phase. As the empty hydrate phase β is generally used as a reference state, the condition results in

$$\Delta\mu^{\beta-L} = \Delta\mu^{\beta-H} \quad (1)$$

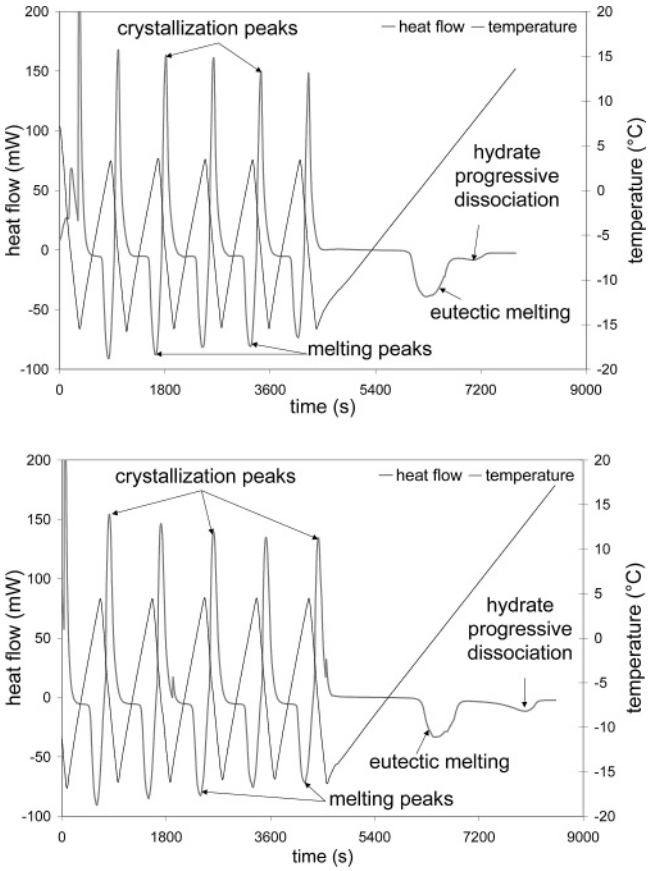

Figure 3. Succession of thermal cycles used to improve the conversion of water−THF (5.97 wt %)−CO_2 solution to CO_2 and (CO_2 + THF) hydrates: top, $P(CO_2) = 0.5$ MPa; bottom, $P(CO_2) = 1.5$ MPa.

The $\Delta\mu^{\beta-L}$ calculation is based on the equation given by Holder et al.[14] considering several contributions expressing the influence of pressure and temperature but also the water activity in the liquid phase,

$$\frac{\Delta\mu^{\beta-L}}{T} = \frac{\Delta\mu_o{}^{\beta-L}}{T} + \frac{P\Delta v^{\beta-L}}{T} + [\Delta h_o{}^{\beta-L} - \Delta C_p{}^{\beta-L}T_{ref}]\left(\frac{1}{T} - \frac{1}{T_{ref}}\right) - \Delta C_p{}^{\beta-L}\ln\frac{T}{T_{ref}} - R\ln a_{H_2O} \quad (2)$$

where the values of parameters $\Delta\mu_o{}^{\beta-L}$, $\Delta v^{\beta-L}$, $\Delta C_p{}^{\beta-L}$, and $\Delta h_o{}^{\beta-L}$ relative to structure I or II are taken from Munck et al.[15]

$\Delta\mu^{\beta-H}$ is evaluated by the expression of van der Waals and Platteeuw,

$$\Delta\mu^{\beta-H} = -RT\sum_{j=\text{cavities}} \nu_j \ln[1 - \sum_{i=\text{species}} \theta_{ij}] \quad (3)$$

where θ_{ij} is the proportion of cavity j occupied by species i. Its calculation involves the C Langmuir parameters, according to

$$\theta_{ij} = \frac{C_{ij}f_i}{1 + \sum_{l=\text{species}} C_{lj}f_l} \quad (4)$$

The fugacity f_i of the hydrate-forming species and the water activity in the liquid mixture involved in eq 2 are calculated using the Redlich−Kwong−Soave equation of state (EOS) associated to the modified Huron−Vidal (MHV2) mixing rule.[16] The advantage of this mixing rule is that it results in a predictive model when combined to a group contribution G^{ex} model such as the modified UNIFAC model.[17]

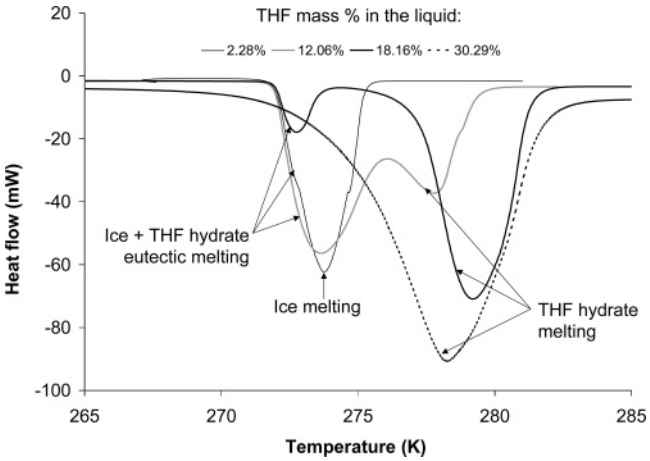

Figure 4. Thermograms obtained with various THF aqueous solutions at atmospheric pressure.

The Langmuir constants C are estimated assuming the following temperature dependence,[18]

$$C = \frac{A}{T}\exp\left(\frac{B}{T}\right) \quad (5)$$

where A and B are constant parameters.

3. Results and Discussion

3.1. DSC Study of L_w−H−V Equilibrium Conditions for Water−THF Systems. To determine the Langmuir parameters A_{THF} and B_{THF} used in the modeling of (CO_2 + THF)-hydrate formation conditions, the water−THF system pressure was studied by DSC at atmospheric pressure. The thermograms recorded upon warming with four different compositions are presented in Figure 4.

At THF concentrations of 2.28, 12.06, and 18.16 wt %, the first peak observed is related to the melting of the eutectic (water + THF hydrate). At 2.28 wt %, it is followed by the ice-melting peak: the two peaks appear partially merged because of the small temperature difference of ~1 K. At 12.06 and 18.16 wt % of THF, the eutectic melting is followed by the melting of the remaining THF hydrate. The equilibrium temperature corresponding to each composition was obtained from the top of the second peak. At 30.29 wt %, no ice is formed, since THF is in excess with respect to the hydrate stoichiometry (19.07 wt %), and the peak is related to the hydrate dissociation.

The experimental temperatures of THF hydrate dissociation, ice melting, and eutectic melting measured for various compositions are reported in Table 1 and illustrated in Figure 5.

3.2. DSC and DTA Study of L_w−H−V Equilibrium Conditions for Water−THF−CO_2 Systems. Experimental results of L_w−H−V equilibrium conditions for water−CO_2 (literature[1] and previous work[4]) and water−THF−CO_2 systems (initial THF concentrations of 5.97, 10.16, and 10.97 wt %) are illustrated in Figure 6 and reported in Table 2. A good consistency was observed between DTA results at 10.97 wt % of THF in water and DSC results at 10.16 wt %.

The experiments showed that adding THF in a water−CO_2 mixture allowed for a significant reduction in the hydrate crystallization pressure. The formation pressures of hydrates formed from water−THF−CO_2 systems fitted from the experimental data and the relative pressure decreases ΔP_{rel} are presented in Table 3, where ΔP_{rel} is defined as the relative

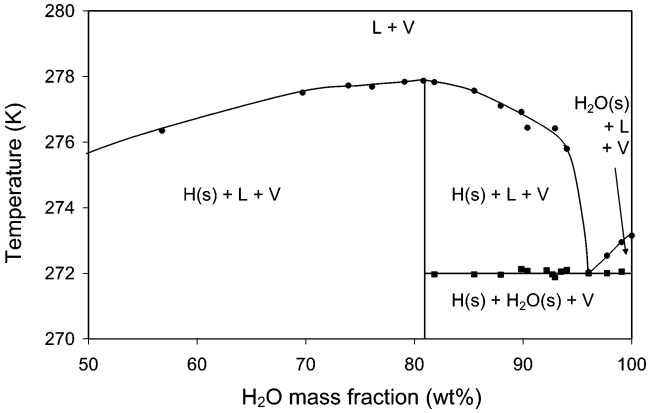

Figure 5. Water−THF phase diagram obtained by DSC experiments.

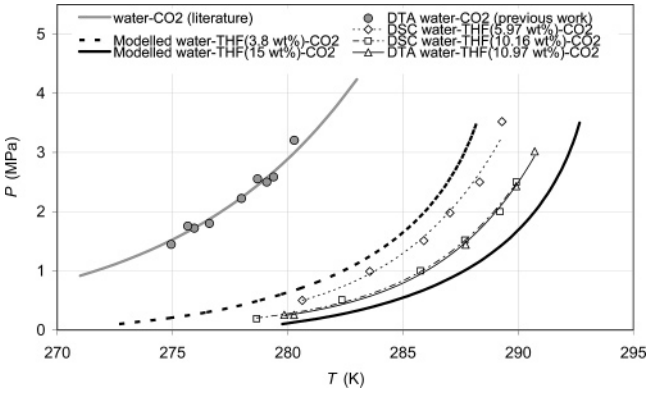

Figure 6. Experimental (DTA and DSC) and modeled L_w-H-V equilibria for water−CO_2 (literature[1] and previous work[4]) and water−THF−CO_2 systems (present work).

Table 1. Experimental (DSC) Temperatures of Hydrate Dissociation, Ice Melting, and Eutectic Melting Measured in THF Solutions at Atmospheric Pressure

	melting temperature (K)		
THF (wt %)	THF hydrate	ice	eutectic
0.00		273.15	
0.93		272.95	272.05
2.28		272.54	272.00
3.98		272.04	272.00
5.97	275.80		272.10
6.50			272.05
7.06	276.42		271.88
7.30			271.97
7.82			272.09
9.60	276.44		272.07
10.16	276.92		272.13
12.06	277.11		271.96
14.49	277.57		271.97
18.16	277.83		271.97
19.17	277.87		
20.90	277.84		
23.90	277.69		
26.08	277.73		
30.29	277.51		

difference between the formation pressure of hydrates formed from water−THF−CO_2 systems and the formation pressure of CO_2 hydrates. For example, at ∼280 K, hydrate can form at a pressure of nearly 0.24 MPa for a water−THF (10.97 wt %)−CO_2 mixture, while single CO_2 hydrate appears at 2.89 MPa, corresponding to a relative pressure decrease of 91.9%. This comparison is considered as possible, since the L_w-H-V equilibrium curve is assumed to be independent from the global

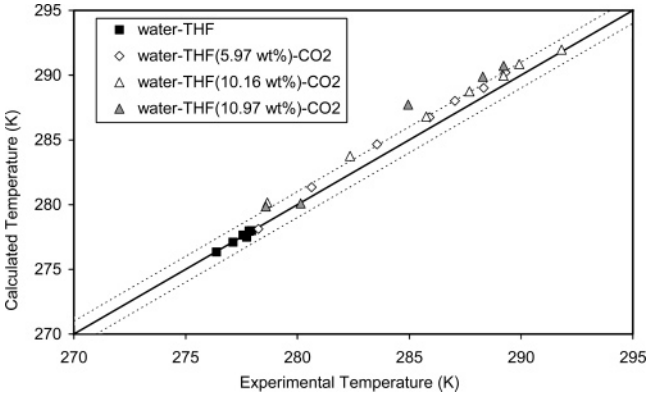

Figure 7. Comparison between predicted and experimental (this work) L_w-H-V equilibrium temperatures of the water−THF−CO_2 system. Dotted lines illustrate deviations of ±1.0 K.

fraction of CO_2 in the multiphase (gas, liquid, and solid) system at the considered experimental conditions.

3.3. Modeling of L_w-H-V Equilibrium Conditions for Water−THF and Water−THF−CO_2 Systems: Experimental Validation and Predictive Results. In a first step, the MHV2 + UNIFAC predictivity was checked by considering the representation of vapor−liquid equilibrium data relative to the water−THF system. The mean relative deviations were 3.1% and 3.9% for isothermal values[19] and for isobaric values,[20] respectively. Isothermal values showed significant deviations between experimental and predicted values only in the case of THF partial pressures calculated at 343.15 K, probably related to the fact that this temperature was close to the lower critical temperature (344.95 K) associated to a liquid−liquid demixing.[21] Nevertheless, this temperature range was far from the L_w-H-V equilibrium temperatures used in refrigeration applications, and the prediction was considered as sufficient to use the model for hydrate-stability calculations.

In a second step, the representation was extended to the stability conditions of pure THF hydrate. Because of their large size, THF molecules form structure II hydrates and only occupy the large cavities of this structure. Hence, only the C_{THF} constant relative to the large cavities of the structure II must be considered. However, no value for this constant was found in the literature. The corresponding parameters were, thus, determined by fitting the data for THF hydrate obtained in the present study. The adjusted values were 6.5972 K/Pa and 1003.22 K for the parameters A_{THF} and B_{THF}, respectively, with very low relative deviations (0.03%).

In the following step, a direct extension of the modeling was applied to the water−THF−CO_2 system and the predicted formation temperatures were compared to the experimental values (Figure 7). In the corresponding calculations, the Langmuir parameter C_{THF} is calculated from eq 5 using the parameters A_{THF} and B_{THF} given above. In the case of C_{CO_2}, values for A and B were given by Parrish and Prausnitz,[18] but also by Munck et al.[15] As $\Delta\mu^{\beta-L}$ was previously evaluated with Munck et al.'s parameters, Munck et al.'s values for A and B were chosen for consistency reasons.

Figure 7 and Table 2 show that the deviations between predicted and experimental equilibrium temperatures are lower than 1.51 K except for one point with a deviation of 3.40 K. The representation of CO_2 solubility used in the modeling over the 0−3.5 MPa pressure range and the 273−373 K temperature range,[22] associated to a 9% relative deviation, could explain the discrepancy. Further calculations are needed to get an

Table 2. Experimental and Modeled (T, P) Conditions of L_w-H-V Equilibrium and Corresponding Dissociation Enthalpy (Clausius−Clapeyron) for Water−CO_2 and Water−THF−CO_2 Systems[a]

water−CO_2 (DTA, previous work)[4]			water−THF (5.97 wt %)−CO_2 (DSC)			
T_{exp} (K)	P_{exp} (MPa)	ΔH (kJ/mol)	T_{exp} (K)	P_{exp} (MPa)	$T_{mod} - T_{exp}$ (K)	ΔH (kJ/mol)
275.0	1.45	77.4	278.3	0.22	−0.1	143.7
275.7	1.76	75.8	280.6	0.50	0.7	141.0
276.0	1.72	76.0	283.6	0.99	1.1	137.5
276.6	1.80	75.6	285.9	1.51	0.8	134.1
278.0	2.22	72.7	287.0	1.98	1.0	128.1
278.7	2.55	70.8	288.3	2.50	0.7	123.3
279.1	2.50	71.2	289.3	3.52	0.9	112.4
279.4	2.59	70.7				
280.3	3.21	66.3				
water−THF (3.8 wt %)−CO_2 (modeling)			water−THF (10.16 wt %)−CO_2 (DSC)			
T_{mod} (K)	P_{mod} (MPa)	ΔH (kJ/mol)	T_{exp} (K)	P_{exp} (MPa)	$T_{mod} - T_{exp}$ (K)	ΔH (kJ/mol)
274.5	0.19	133.0	278.7	0.19	1.5	147.4
278.3	0.45	131.0	282.4	0.51	1.4	144.5
283.5	1.22	125.2	285.8	1.00	1.0	140.5
286.8	2.40	114.5	287.7	1.52	1.1	135.7
287.7	3.00	109.4	289.2	2.00	0.7	131.3
			289.9	2.50	0.9	126.2
water−THF (15 wt %)−CO_2 (modeling)			water−THF (10.97 wt %)−CO_2 (DTA)			
T_{mod} (K)	P_{mod} (MPa)	ΔH (kJ/mol)	T_{exp} (K)	P_{exp} (MPa)	$T_{mod} - T_{exp}$ (K)	ΔH (kJ/mol)
282.9	0.32	160.9	279.9	0.26	1.5	156.0
285.0	0.55	158.7	280.1	0.26	3.4	156.0
289.5	1.50	149.8	287.7	1.44	1.0	145.5
291.6	2.50	139.9	289.9	2.43	1.1	134.9
292.4	3.20	132.1	290.7	3.02	1.1	129.2

[a] Deviations between modeled and experimental temperatures values are given for initial THF concentrations of 5.97, 10.16, and 10.97 wt %.

Table 3. Fitted Formation Pressures of Hydrates Formed from Water−THF−CO_2 Systems and Relative Pressure Decrease ΔP_{rel}

		water−THF (x wt %)−CO_2 system									
		$x = 3.8$		$x = 5.97$		$x = 10.16$		$x = 10.97$		$x = 15$	
T (K)	$P_{CO_2\ hydrate}$ (MPa)	P (MPa)	ΔP_{rel} (%)	P (MPa)	ΔP_{rel} (%)	P (MPa)	ΔP_{rel} (%)	P (MPa)	ΔP_{rel} (%)	P (MPa)	ΔP_{rel} (%)
274	1.345	0.178	86.8	0.120	91.1	0.073	94.6	0.057	95.7	0.038	97.1
275	1.527	0.218	85.7	0.149	90.3	0.091	94.1	0.073	95.2	0.049	96.8
276	1.735	0.268	84.6	0.184	89.4	0.113	93.5	0.092	94.7	0.062	96.4
277	1.971	0.329	83.3	0.229	88.4	0.141	92.8	0.116	94.1	0.079	96.0
278	2.239	0.404	81.9	0.284	87.3	0.176	92.1	0.147	93.4	0.100	95.5
279	2.543	0.496	80.5	0.353	86.1	0.220	91.4	0.186	92.7	0.127	95.0
280	2.889	0.610	78.9	0.438	84.8	0.275	90.5	0.235	91.9	0.161	94.4
281	3.282	0.749	77.2	0.544	83.4	0.343	89.6	0.297	90.9	0.204	93.8
282	3.728	0.919	75.3	0.675	81.9	0.428	88.5	0.376	89.9	0.259	93.1
283	4.235	1.129	73.3	0.838	80.2	0.534	87.4	0.476	88.8	0.329	92.2
284	4.810	1.387	71.2	1.040	78.4	0.667	86.1	0.602	87.5	0.417	91.3
285	5.464	1.703	68.8	1.292	76.4	0.832	84.8	0.761	86.1	0.529	90.3

unambiguous explanation of the discrepancy between predicted and experimental equilibrium temperatures.

The model was extended to lower and higher THF concentrations. Predictive results of L_w-H-V equilibrium conditions for water−THF (3.8 wt %)−CO_2 and water−THF (15 wt %)−CO_2 systems are presented in Figure 6 and reported in Table 2. A good consistency is observed, since the hydrate-formation pressure relative to the water−THF (3.8 wt %)−CO_2 system is higher than that relative to the other systems. Reciprocally, the hydrate-formation pressure relative to water−THF (15 wt %)−CO_2 systems is lower than that relative to the other systems.

Other predicted formation pressures of hydrates formed from water−THF−CO_2 systems and the corresponding relative pressure decreases ΔP_{rel} are presented in Table 3, to be compared at the same temperatures to the values fitted from the experimental data.

3.4. Dissociation Enthalpy Calculation Based on Experimental and Predicted Equilibrium Data. Table 2 and Figure 8 give the molar dissociation enthalpy of the hydrates formed from water−CO_2 and water−THF−CO_2 systems, calculated from experimental equilibrium data (previous work[4] and present

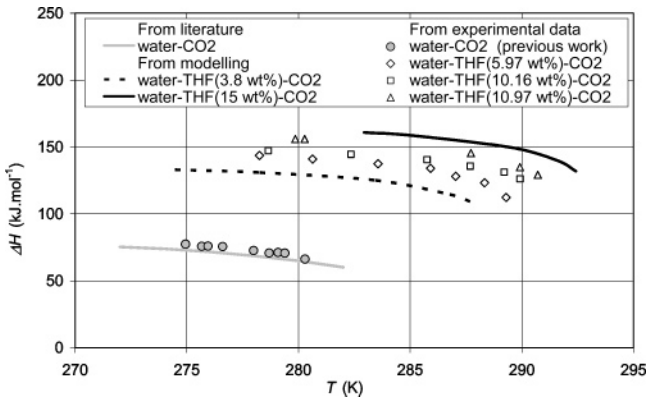

Figure 8. Dissociation enthalpy of hydrates formed from water−CO_2 and water−THF−CO_2 systems calculated by the Clausius−Clapeyron equation based on literature,[1] modeling (present work), and experimental data (previous work[4] and present work).

Table 4. Dissociation Enthalpies of Hydrates Formed from Water−THF−CO_2 Systems with Various Initial THF Concentrations (3.18, 5.97, 10.16, 10.97, and 15 wt %) and Corresponding Dissociation Enthalpy Ratios *k* at 280 K (Based on $\Delta H_{CO_2\ hydrate} = 65$ kJ/mol)

initial THF concentration (wt %)	$\Delta H_{THF-CO_2\ hydrate}$ (kJ/mol)	*k*
3.8	130	2.0
5.97	142	2.2
10.16	147	2.3
10.97	155	2.4
15	163	2.5

work) and modeling (present work) using the Clausius−Clapeyron equation,[13]

$$\frac{\mathrm{d}\ln P}{\mathrm{d}(1/T)} = -\frac{\Delta \mathrm{H}}{zR} \tag{6}$$

where ΔH was expressed in J/mol_{CO_2} consumed by the hydrate formation and z was given by the Nelson−Obert charts.[23]

First of all, as shown in Figure 8, the CO_2-hydrate dissociation enthalpy ($\Delta H_{CO_2\ hydrate}$) at 280.3 K is in good agreement with the value of 65.22 kJ/mol measured by Kang et al.[2] Figure 8 shows that the molar dissociation enthalpy of the hydrate formed from water−THF−CO_2 systems, noted $\Delta H_{THF-CO_2\ hydrate}$, is higher than $\Delta H_{CO_2\ hydrate}$. Table 4 gives at 280 K the values of $\Delta H_{THF-CO_2\ hydrate}$ and the ratios k between $\Delta H_{THF-CO_2\ hydrate}$ and $\Delta H_{CO_2\ hydrate}$ defined as

$$k = \frac{\Delta H_{THF-CO_2\ hydrate}}{\Delta H_{CO_2\ hydrate}} \tag{7}$$

Table 4 shows that the molar dissociation enthalpy of the solid formed with initial THF concentrations in water from 3.8 to 15 wt % increases k from 2.0 to 2.5. The high values of $\Delta H_{THF-CO_2\ hydrate}$ are likely to be attributable to a hydrate structure change (from structure I to structure II or from structure I to a mixture of structures I and II).

4. Conclusion and Perspectives

In the present study, hydrate-formation conditions were experimentally investigated on water−THF−CO_2 systems using differential thermal analysis (DTA) and differential scanning calorimetry (DSC) devices. A good agreement was observed between DTA and DSC experiments. In addition, a modeling of hydrate-formation conditions was developed for water−THF−CO_2 systems. The deviations associated to the modeling of equilibrium temperatures were consistent with experimental deviations. The first main result of this work was that the hydrates formed from water−THF−CO_2 systems have significantly lower equilibrium pressures than the CO_2 hydrates. For example, an average relative pressure decrease of 79% was observed for the considered temperature range (274−285 K) at a low initial concentration of THF in water (3.8 wt %). Moreover, the use of the Clausius−Clapeyron equation, based on experimental and predictive equilibrium data, allowed us to calculate hydrate dissociation enthalpies. The results for the dissociation enthalpies of hydrates formed from water−THF−CO_2 systems were roughly two times higher than the results for the dissociation enthalpies of CO_2 hydrates. This study confirmed the interest of adding THF to water−CO_2 systems, even in small quantities, to form a mixed-hydrate slurry suitable for secondary refrigeration. Further experiments based on Raman spectroscopy are currently being carried out in order to investigate the hydrate structures formed from water−THF−CO_2 systems and the cavity occupation rate. These data are necessary to describe the mechanisms related to (CO_2 + THF)-hydrate formation and, thus, to give explanations about the equilibrium pressure and dissociation enthalpy values.

Nomenclature

a_{H_2O} = activity in water
A = parameter expressing Langmuir constants temperature dependence, K/Pa
B = parameter expressing Langmuir constants temperature dependence, K
C_{ij} = Langmuir constant for component i in cavity j, 1/Pa
(L_w−H−V) = liquid−hydrate−vapor
f_i = fugacity for component i, Pa
k = ratio between $\Delta H_{THF-CO_2\ hydrate}$ and $\Delta H_{CO_2\ hydrate}$
P = pressure, Pa
$P_{CO_2\ hydrate}$ = CO_2-hydrate formation pressure, Pa
R = universal gas constant, J/(mol·K)
T = temperature, K
T_{ref} = reference temperature, K
x = initial concentration of THF in water, wt %
z = gas compressibility

Greek Letters

$\Delta C_p^{\beta-L}$ = water heat capacity difference between the empty hydrate β and liquid phases, J/(mol·K)
ΔH = dissociation enthalpy, J/mol_{CO_2}
$\Delta H_{CO_2\ hydrate}$ = CO_2 hydrate dissociation enthalpy, J/mol_{CO_2}
$\Delta H_{THF-CO_2\ hydrate}$ = dissociation enthalpy of the solid formed from water−THF−CO_2 systems, J/mol_{CO_2}
$\Delta h_o^{\beta-L}$ = water enthalpy difference between the empty hydrate β and liquid phases at reference temperature and zero absolute pressure, J/mol
$\Delta\mu^{\beta-H}$ = water chemical potential difference between the empty hydrate β and hydrate phases, J/mol
$\Delta\mu^{\beta-L}$ = water chemical potential difference between the empty hydrate β and liquid phases, J/mol
$\Delta\mu_o^{\beta-L}$ = water chemical potential difference between the empty hydrate β and liquid phases at reference temperature and zero absolute pressure, J/mol
ΔP_{rel} = relative pressure decrease between formation pressure of hydrates formed from water−THF−CO_2 systems and formation pressure of CO_2 hydrates
$\Delta v^{\beta-L}$ = water volume difference between the empty hydrate β and liquid phases, m^3/mol
v_j = number of type j cavities per water molecule in unit cell
θ_{ij} = fractional occupation of cavity j by component i

Literature Cited

(1) Sloan, E. D. *Clathrate Hydrate of Natural Gases*, 2nd ed.; Dekker: New York, 1998.

(2) Kang, S. P.; Lee, H.; Ryu, B. J. Enthalpies of Dissociation of Clathrate Hydrates of Carbon Dioxide, Nitrogen, (Carbon Dioxide + Nitrogen), and (Carbon Dioxide + Nitrogen + Tetrahydrofuran). *J. Chem. Thermodyn.* **2001**, *33*, 513−521.

(3) Seo, Y.-T.; Lee, H. Structure and Guest Distribution of the Mixed Carbon Dioxide and Nitrogen Hydrates as Revealed by X-ray Diffraction and ^{13}C NMR Spectroscopy. *J. Phys. Chem. B* **2004**, *108*, 530−534.

(4) Fournaison, L.; Delahaye, A.; Chatti, I.; Petitet, J.-P. CO_2 Hydrates in Refrigeration Processes. *Ind. Eng. Chem. Res.* **2004**, *43*, 6521−6526.

(5) Marinhas, S.; Fournaison, L.; Delahaye, A.; Chatti, I.; Petitet, J.-P. Valorisation Énergétique des Hydrates de Gaz Appliquée à la Réfrigération et la Climatisation. In *Proceedings of the SFT 2004*, Giens, France, 2004; pp 915−920.

(6) Akiya, T.; Shimazaki, T.; Oowa, M.; Nakaiwa, M.; Nakane, T.; Usuda, T.; Ebinuma, T.; Kamesaki, K. Formation Characteristics of Tetrahydrofuran Hydrate to Be Used as a Cool Storage Medium. In *Proceedings of the 62nd Annual Meeting of the Society of Chemical Engineers*, Tokyo, Japan, 1997; p 174.

(7) Iida, T.; Mori, H.; Mochizuki, T.; Mori, Y. H. Formation and Dissociation of Clathrate Hydrate in Stoichiometric Tetrahydrofuran−Water Mixture Subjected to One-Dimensional Cooling or Heating. *Chem. Eng. Sci.* **2001**, *56*, 4747−4758.

(8) Gough, S. R.; Davidson, D. W. Composition of Tetrahydrofuran Hydrate and the Effect of Pressure on the Decomposition. *Can. J. Chem.* **1971**, *49*, 2691−2699.

(9) Dyadin, Y. A.; Kuznetsov, P. N.; Yakovlev, I. I.; Pyrinova, A. V. *Dokl. Akad. Nauk. SSSR* **1973**, *208*, 103−106.

(10) Hanley, H. J. M.; Meyers, G. J.; White, J. W.; Sloan, E. D. The Melting Curve of Tetrahydrofuran Hydrate in D_2O. *Int. J. Thermophys.* **1989**, *10*, 903−909.

(11) Otake, K.; Tsuji, T.; Sato, I.; Akiya, T.; Sako, T.; Hongo, M. U. A Proposal of a New Technique for the Density Measurement of Solids. *Fluid Phase Equilib.* **2000**, *171*, 175−179.

(12) van der Waals, J. H.; Platteeuw, J. C. Clathrate Solution. *Adv. Chem. Phys.* **1959**, *2*, 1−57.

(13) Sloan, E. D. J.; Fleyfel, F. Hydrate Dissociation Enthalpy and Guest Size. *Fluid Phase Equilib.* **1992**, *76*, 123−140.

(14) Holder, G. D.; Corbin, G.; Papadopoulos, K. D. Thermodynamic and Molecular Properties of Gas Hydrates from Mixtures Containing Methane, Argon, and Krypton. *Ind. Eng. Chem. Fundam.* **1980**, *19*, 282−286.

(15) Munck, J.; Skjold-Jorgensen, S.; Rasmussen, P. Computations of the Formation of Gas Hydrates. *Chem. Eng. Sci.* **1988**, *43*, 2661−2672.

(16) Dahl, S.; Fredenslund, A.; Rasmussen, P. The MHV2 Model: A Unifac-Based Equation of State Model for Prediction of Gas Solubility and Vapor−Liquid Equilibria at Low and High Pressures. *Ind. Eng. Chem. Res.* **1991**, *30*, 1936−1945.

(17) Larsen, B. L.; Rasmussen, P.; Fredenslund, A. A Modified UNIFAC Group-Contribution Model for Prediction of Phase Equilibria and Heats of Mixing. *Ind. Eng. Chem. Res.* **1987**, *26*, 2274−2286.

(18) Parrish, W. R.; Prausnitz, J. M. Dissociation Pressures of Gas Hydrates Formed by Gas Mixtures. *Ind. Eng. Chem. Process Des. Dev.* **1972**, *11*, 26−34.

(19) Matous, J.; Hrncirik, J.; Novak, J.; Sobr, J. *Collect. Czech. Chem. Commun.* **1972**, *37*, 2653−2663.

(20) Shnitko, V. A.; Kogan, V. B. *Zh. Prikl. Khim.* **1969**, *41*, 1305−1313.

(21) Matous, J.; Hrncirik, J.; Novak, J.; Sobr, J. *Collect. Czech. Chem. Commun.* **1970**, *35*, 1904−1905.

(22) Houghton, G.; McLean, A. M.; Ritchie, P. D. Compressibility, Fugacity, and Water-Solubility of Carbon Dioxide in the Region 0−36 atm and 0−100 °C. *Chem. Eng. Sci.* **1957**, *6*, 132−137.

(23) Çengel, Y. A.; Boles, M. A. *Thermodynamics: An Engineering Approach*, 4th ed.; Boston, MA, 2002.

Received for review March 17, 2005
Revised manuscript received October 13, 2005
Accepted October 14, 2005

IE050356P